ACS OMEGA

http://pubs.acs.org/journal/acsodf

Article

Non Noble-Metal Copper–Cobalt Bimetallic Catalyst for Efficient Catalysis of the Hydrogenolysis of 5-Hydroxymethylfurfural to 2,5-Dimethylfuran under Mild Conditions

Qingtu Zhang, Jianliang Zuo,* Lu Wang, Feng Peng, Shengzhou Chen, and Zili Liu*

Cite This: *ACS Omega* 2021, 6, 10910–10920

Read Online

ACCESS | Metrics & More | Article Recommendations | Supporting Information

ABSTRACT: The efficient catalysis of the hydrogenation of 5-hydroxymethylfurfural (HMF) to 2,5-dimethylfuran (DMF) over non noble-metal catalysts has received great attention in recent years. However, the reaction usually requires harsh conditions, such as high reaction temperature and excessively long reaction time, which limits the application of the non noble-metal catalysts. In this work, a bimetallic Co_x-Cu@C catalyst was prepared via the pyrolysis of MOFs, and an 85% DMF yield was achieved under a reaction temperature and time of 160 °C and 3 h, respectively. The results of X-ray diffraction (XRD), X-ray photoelectron spectroscopy (XPS), energy-dispersive X-ray spectroscopy (EDX) mapping, and other characterization techniques showed that the synthesis method in this paper realized the in situ loading of cobalt into the copper catalyst. The reaction mechanism studies revealed that the cobalt doping effectively enhanced the hydrogenation activity of the copper-based catalyst on the C–O bond at a low temperature. Moreover, the bimetallic Co_x-Cu@C catalyst exhibited superior reusability without any loss in the activity when subjected to five testing rounds.

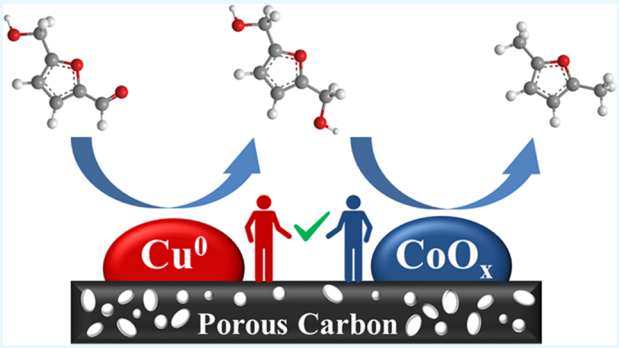

INTRODUCTION

The demand for energy in modern society is rapidly increasing with economic and social developments. Problems such as limited fossil reserves and environmental pollution caused by fossil fuel combustion are becoming increasingly critical.[1,2] Therefore, it is urgent to seek a renewable energy source to gradually replace fossil energy sources.[3] Biomass, with abundant reserves, is easily converted into liquid fuel and is expected to gradually replace the use of commercial fuel, even faster than other renewable energy sources such as wind energy and solar energy.[4−6] The popular biomass-derived platform compound 5-hydroxymethylfurfural (HMF), obtained from lignocellulose and other carbohydrates, can be transformed into a high-quality biofuel 2,5-dimethylfuran (DMF). This biofuel is regarded as an alternative to commercial gasoline owing to its many excellent physical and chemical properties, including high energy density, high octane number, and high stability.[7−12]

However, the conversion of HMF into DMF requires the selective hydrogenolysis of aldehyde groups and hydroxymethyl on HMF while protecting other functional groups to achieve an efficient and highly selective conversion, and this presents certain challenges.[13,14] Noble-metal catalysts such as Pd[15] and Ru[16] show good activity but have a high cost. Currently, the development of copper, a non noble-metal catalyst, for HMF hydrogenation has received attention, owing to its low cost and relatively high selectivity. Brzezinska et al. reported a CuZnO catalyst applied in HMF hydrogenation to produce DMF, and the catalyst could achieve a DMF selectivity of up to 94% at 220 °C reaction temperature.[17] Esteves et al. used a variety of supports to prepare supported copper catalysts for the selective hydrogenation of HMF; the Cu/Al_2O_3 catalyst could achieve 90% DMF selectivity at a reaction temperature of 150 °C, but the required reaction time was 10 h.[18] Sarkar et al. reported a Cu-Pd@C catalyst obtained from the pyrolysis of Cu-MOFs. The catalyst achieved 96% DMF selectivity under very mild reaction conditions (120 °C for 7 h) for HMF hydrogenation.[15] In this reaction system, noble metals play an important role. For copper-based catalysts without noble metals, it is difficult to achieve the HMF conversion to DMF at a low temperature in a short time.

Numerous studies have shown that copper-based catalysts have high selectivity for HMF conversion to DMF.[19−21] However, copper-based catalysts without noble metals exhibit low hydrogenation activity for the C–O bond; consequently,

Received: February 5, 2021
Accepted: April 5, 2021
Published: April 16, 2021

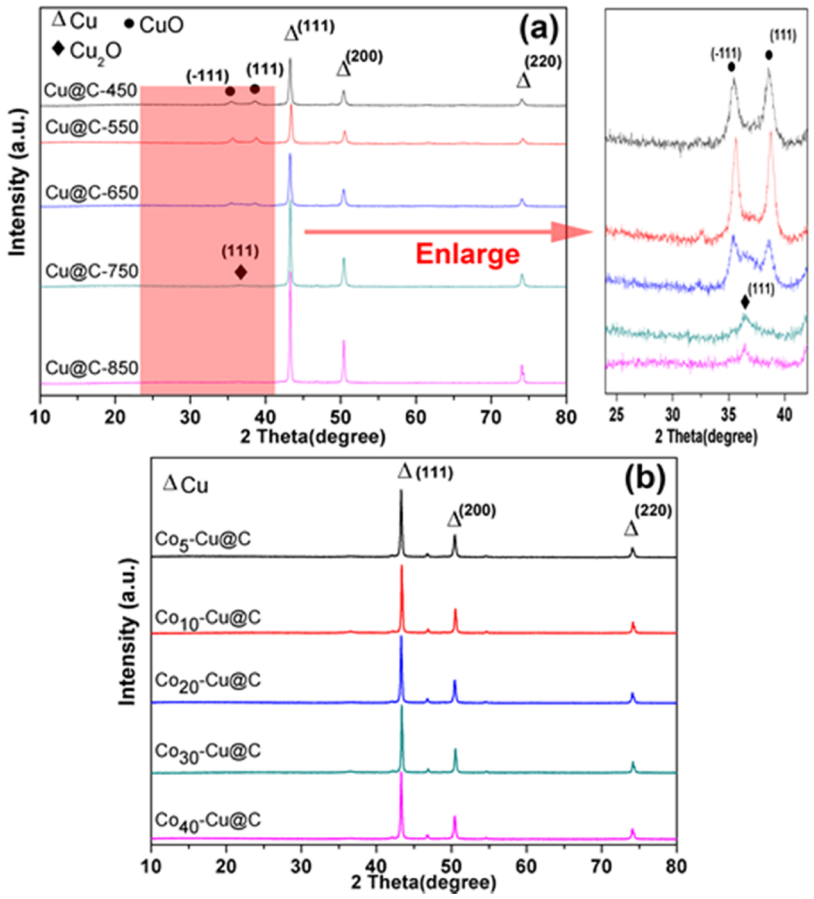

Figure 1. X-ray diffraction patterns of (a) Cu@C-X and (b) Co_x-Cu@C catalysts.

the HMF hydrogenation requires higher reaction temperatures (usually above 180 °C) or excessively long reaction times (usually more than 8 h) for the intermediate products such as 2,5-dihydroxymethylfuran (DHMF) to convert to DMF.

In recent years, catalysts derived from pyrolysis of metal−organic frameworks (MOFs) have shown excellent catalytic activity.[22,23] The MOF-derived catalysts have attracted considerable attention because of their excellent activity in catalytic hydrogenation.[24,25] Herein, we report the development of a copper-based bimetallic catalyst derived from MOFs for the selective hydrogenation of 5-HMF to DMF under mild conditions. High-resolution transmission electron microscopy, energy-dispersive X-ray spectroscopy (EDX), X-ray diffraction (XRD), and X-ray photoelectron spectroscopy (XPS) were utilized to study the physical and surface properties of the catalyst. The cobalt doping was found to effectively promote the catalyst hydrogenation activity on the C−O bond. Under the optimal conditions, the catalyst achieved 100% HMF conversion and over 85% DMF yield under a reaction temperature and time of 160 °C after 3 h, respectively, and exhibited excellent recyclability.

RESULTS AND DISCUSSION

Catalyst Structure Characterization. The XRD patterns of the Cu-MOFs and Co-Cu-MOFs (Figure S1) show Cu_3BTC_2 (BTC: 1,3,5-benzenetricarboxylic acid) crystal diffraction peaks (2θ = 11.6, 13.4, 17.5, 19.0°),[26] indicating that Cu_3BTC_2 MOFs were successfully synthesized through this method. No new diffraction peak occurred in the XRD pattern of Co-Cu-MOFs compared with that of Cu-MOFs, indicating that cobalt was probably only loaded into Cu_3BTC_2 and that a new crystal structure was not formed, which was further confirmed via Fourier transform infrared spectroscopy analysis (Figure S2) of the precursor; the analysis results revealed that no new functional groups were formed on the Co-Cu_3BTc_2 precursor.

Furthermore, Cu-MOF catalysts derived under different pyrolysis temperatures were analyzed via XRD. Strong Cu diffraction peaks (2θ = 43.2°, 50.3°, 73.9°, ICSD: 70-3038) could be detected in all catalysts (Figure 1a), suggesting that most of the copper in the catalysts was reduced to Cu^0 after pyrolysis. However, weak CuO diffraction peaks (2θ = 35.6°, 38.8°, ICSD: 89-5899) were detected when the pyrolysis temperature was relatively low. As the pyrolysis temperature increased, CuO reduced to form Cu_2O, and the diffraction peak of Cu_2O (2θ = 36.4°, 42.3°, ICSD: 78-2076) increased. However, no diffraction peaks of Co or Co oxides occurred in the XRD patterns of the Co_x-Cu@C catalyst (Figure 1b) because the Co in the catalyst was highly dispersed and low in content, which accords with the inductively coupled plasma−atomic emission spectroscopy results (Table 1).

The nitrogen adsorption−desorption curves of the MOF-derived catalysts are of type IV with sharp adsorption in a relatively low pressure region (Figure S3), indicating the existence of micropores and mesoporous structures. The catalyst pore structure parameters are presented in Table S1. All of the catalysts showed a high specific surface area. When materials are highly porous, the diffusion rates of the substrates and the products are likely to be faster than the catalytic rate. As the pyrolysis temperature increased, the specific surface area

https://doi.org/10.1021/acsomega.1c00676
ACS Omega 2021, 6, 10910−10920

Table 1. Elemental Content of Catalysts

catalyst	Cu elemental content (wt %)	Co elemental content (wt %)	Co/Cu molar ratio (%)
Cu@C-750	67.3	0	
Co_5-Cu@C	70.8	0.19	0.25
Co_{10}-Cu@C	67.8	0.38	0.52
Co_{20}-Cu@C	65.7	0.67	0.94
Co_{30}-Cu@C	62.2	0.83	1.23
Co_{40}-Cu@C	62.3	1.15	1.70

of the catalyst decreased, since the carbon structure of the catalyst collapsed at high temperatures. For the Co-doped catalysts, when the Co doping amount increased, both the catalyst surface area and pore size decreased, which is the result of the cobalt aggregation.

Figure 2 shows the electron microscopy analysis results of the MOF and MOF-derived catalysts. As shown in Figure 2a, the precursor has a typical octahedral structure, which agrees with relevant literature reports.[27,28] The Cu_3BTC_2 synthesized via the static precipitation method had a smaller particle diameter, about 1−2 μm, than that synthesized via the traditional hydrothermal method.[29] Also, there were no obvious differences in the shapes of the precursor before and after cobalt doping (Figure S5). After the pyrolysis treatment, the catalyst morphology significantly changed. The structure was transformed into an octahedral matrix embedded with spheres, and the diameter of the spheres was about 150 nm. The EDX mapping profiles (Figure 2d−f) of the catalyst showed strong copper signals around the sphere; the ball may be copper particles. Moreover, based on the signal distribution, the Co element was uniformly and highly dispersed on the catalyst.

The transmission electron microscopy image of the catalyst (Figure 2g−i) shows that the sphere was embedded in the octahedron. A significant contrast existed between the octahedral matrix and the spherical particles because the octahedral matrix mainly had a carbonaceous structure, and the spheres were metal particles. In addition, further magnification of the sphere revealed that the particles were covered with a carbonaceous shell; this finding is consistent with the results in the literature.[30] Based on the above characterization analysis results, a schematic diagram of the structural changes during the catalyst synthesis process is presented in Scheme 1.

Figure 3 displays the XPS results of the catalyst. Figure 3a shows strong Cu 2p, C 1s, N 1s, and O 1s peaks and a weak Co peak. The high-resolution spectrum of Cu 2p (Figure 3c) shows a peak of Cu $2p_{3/2}$ near 934 eV, which is decomposed into two peaks at 934.1 and 932.2 eV, corresponding to Cu^{2+} and Cu^0/Cu^+, respectively.[31−33] The ratio of the peaks of Cu^+/Cu^0 and Cu^{2+} has been calculated and shown in Table S2. Similarly, in the Auger spectrum of Cu LMM (Figure 3d), peaks at 913.1, 917.1, and 920.8 eV correspond to Cu^+, Cu^{2+}, and Cu^0, respectively.[34,35] The doublet separation between the $2p_{3/2}$ and $2p_{1/2}$ signals approaches 15.5 eV (Figure 3b), which agrees with the standard spectra of elemental cobalt, suggesting the existence of Co^{3+} or Co^{2+} species.[36] The satellite peak at 789.6 eV corresponds to Co^{2+}, and the peaks at 785.2 and

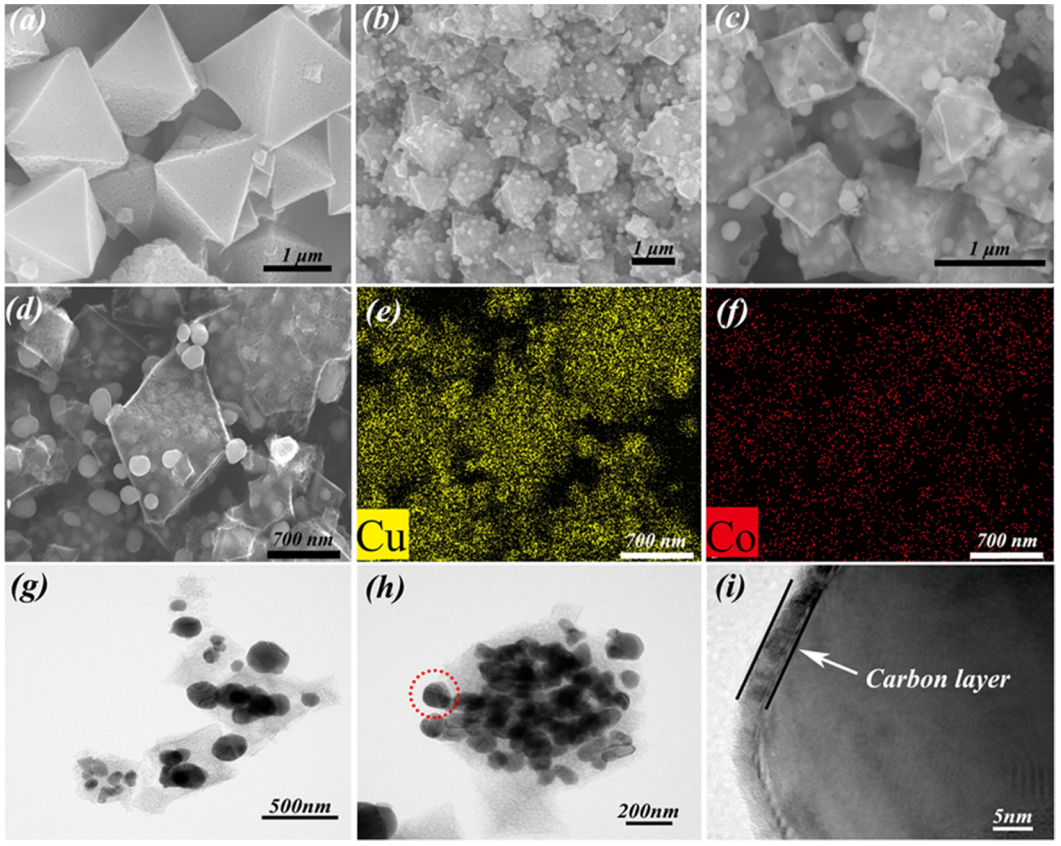

Figure 2. Electron microscopy characterizations for the catalyst: (a−c) scanning electron microscopy images of the Cu_3BTC_2 precursor, Cu@C-750, and Co_{20}-Cu@C, respectively; (d−f) energy-dispersive X-ray spectroscopy mapping profiles of Co_{20}-Cu@C; and (g−i) high-resolution transmission electron microscopy images of Co_{20}-Cu@C.

https://doi.org/10.1021/acsomega.1c00676
ACS Omega 2021, 6, 10910−10920

Scheme 1. Schematic Illustration of the Synthesis of Co_x-Cu@C and Its Application in HMF Selective Hydrogenation

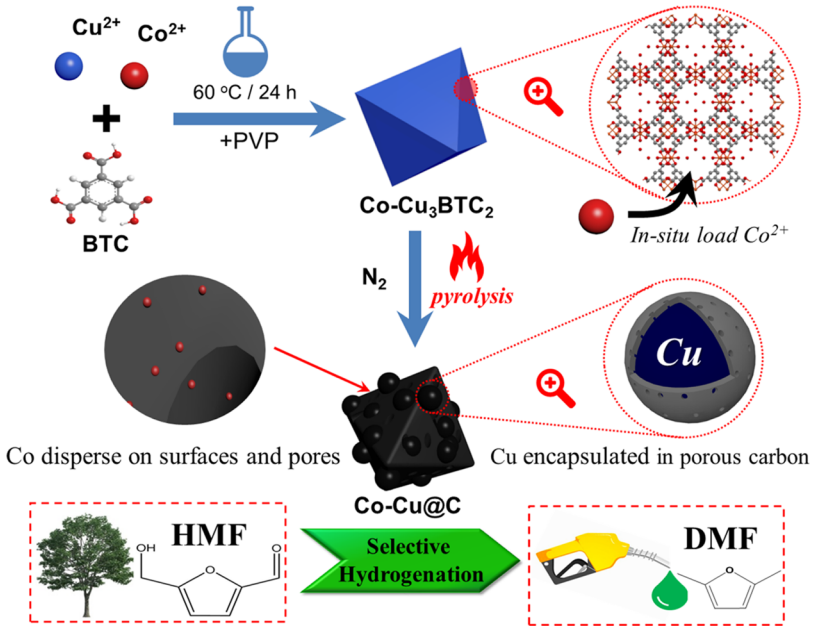

780.5 eV correspond to the binding energies of Co^{2+} and Co^{3+}, respectively, indicating that cobalt exists mainly in the form of oxides.[37−39]

Furthermore, the C 1s high-resolution XPS spectrum of the catalyst (Figure 3e) shows a sharp peak at 284.4eV, caused by the hybridization of C sp^2 and C sp^3, which are mainly from the carbon structure of the catalyst. The wide peak near 289 eV corresponds to carbon nitride, indicating that the added PVP still retained a small amount of nitrogen in the catalyst after a high-temperature treatment.[40,41] To further confirm the form of carbon in the catalyst, the catalyst was characterized via Raman spectroscopy. As shown in Figure S4, D and G bands were detected, and the I_G/I_D ratio of the catalyst was less than 1, indicating that the carbon in the catalyst had a higher graphitization degree. From the N 1s high-resolution spectrum (Figure 3f), except for the nitrogen that formed carbon nitride, most of the nitrogen atoms remained in the catalyst as constituents of heterocyclic compounds.[42]

As shown in the Cu 2p high-resolution XPS spectrum and Auger spectrum, the undoped and doped catalysts had similar photoelectron binding energies and kinetic energies, and they also had similar atomic ratios, indicating that the Co doping had no significant effect on the chemical environment of copper. The C 1s and N 1s high-resolution XPS spectra of the catalyst were similar, which also shows that cobalt doping had little effect on the catalyst surface properties.

In summary, the above characterization results indicate that the precursor did not form new crystals or functional groups after cobalt doping; the cobalt was probably only loaded into the precursor. The XRD and XPS results indicate that the copper in the catalyst mainly existed as Cu^0 species and a small amount existed as Cu^+ species, while the cobalt mainly existed as CoO_x. According to the results of nitrogen adsorption−desorption and electron microscopy analysis, cobalt doping had no significant effect on the catalyst structure. Moreover, the XPS survey results show that cobalt doping did not significantly change the chemical environment of copper in the catalyst. Therefore, the Cu and CoO_x nanoparticles may act as relatively independent active sites and play different roles in the catalytic process.

Catalytic Performance in Selective Hydrogenation of HMF. First, the effect of the pyrolysis temperature of the catalyst on the catalyst activity was studied. Different monometallic catalysts were prepared via precursor pyrolysis under different temperatures: 450, 550, 650, 750, and 850 °C. The results of the catalytic performance (Figure 4) depicted that almost all of the catalysts showed 100% HMF conversion. The catalyst prepared at 750 °C achieved the highest DMF yield of 92%. According to the above XRD analysis, this high DMF yield was due to the conversion of CuO to Cu_2O as the pyrolysis temperature increased. Previous studies have reported that Cu^+ species play an important role in the hydrogenation of HMF.[29,43,44] Therefore, in this study on a bimetallic catalyst, the pyrolysis temperature of 750 °C was used for the catalyst preparation.

The monometallic catalyst achieved 100% HMF conversion and a 92% DMF yield, but the reaction required a temperature of 180 °C and a time of 4 h. However, our previous research has proved that the activity of the monometallic catalyst significantly decreases after a reaction.[29]

To enhance the catalyst stability and further reduce the requirements of the reaction conditions, metal doping is used to modulate the catalyst performance. The catalysts were separately doped with Co, Zn, and Ni. The corresponding catalysts were synthesized, and their activities were evaluated.

The results of catalytic performance are illustrated in Figure 5, compared with the performances of monometallic catalysts. The activity of the metal-doped catalysts was significantly improved. Cobalt doping had the most significant effect on the catalyst activity, with the DMF yield higher than that of the monometallic catalyst by 29.4%.

Subsequently, the cobalt doping amount was optimized, and catalysts with cobalt doping amounts of 5, 10, 20, 30, and 40% were synthesized. The catalytic performance results are illustrated in Figure 6. When the cobalt doping amount increased, the DMF yield first increased and then decreased. When the Co doping amount is too low, the rare CoO_x sites

https://doi.org/10.1021/acsomega.1c00676
ACS Omega 2021, 6, 10910−10920

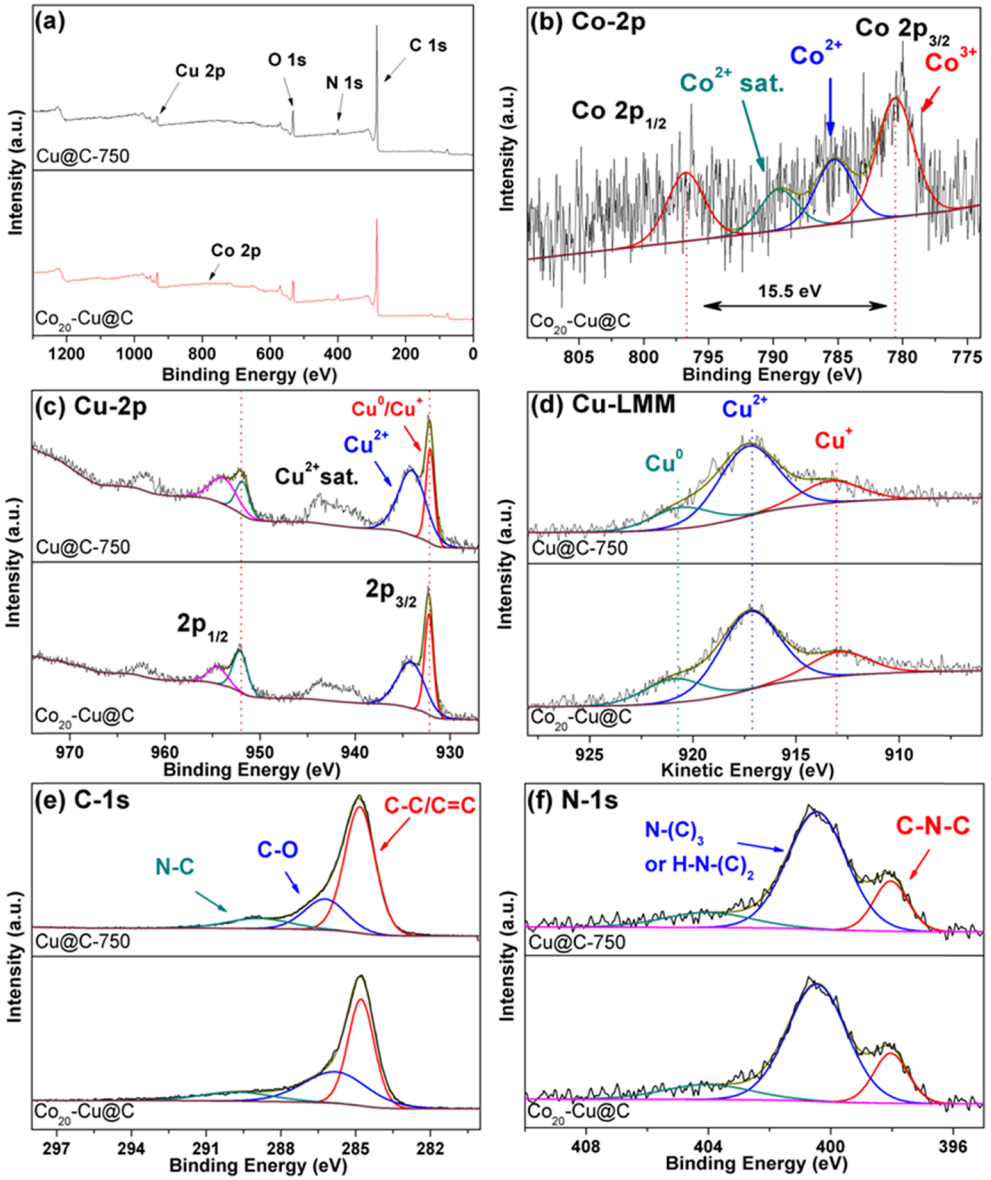

Figure 3. (a) X-ray photoelectron spectroscopy survey results; (b, c, e, f) high-resolution spectra of Co 2p, Cu 2p, C 1s, and N 1s, respectively; and (d) Cu LMM Auger spectrum.

cannot effectively activate the C−O bond. However, excessive amounts of cobalt may accumulate and block the pores of the catalyst. When the doping amount was 20%, the maximum yield was obtained.

To research the effect of cobalt doping on catalyst activity, the catalytic performances of Co_{20}-Cu@C and Cu@C-N750 catalysts in the selective hydrogenation of HMF at different temperatures were investigated. As shown in Figure 7, at low temperatures, the Co_{20}-Cu@C catalyst showed higher yields of DMF and 2,5-dimethyltetrahydrofuran (DMTHF) than Cu@C-N750. At 180 °C, both catalysts showed similar activity results. This finding indicates that the cobalt doping modulated the low-temperature catalytic activity of the catalyst.

In addition, we optimized the reaction time (Table S4). After 3 h of reaction, an 85% yield of DMF could be obtained. The reaction time was further extended to 4−6 h, and the DMF yield did not significantly increase.

In summary, the research on the reaction conditions of catalytic hydrogenation shows that the Co_{20}-Cu@C catalyst could achieve the best activity results under 160 °C and 3 h reaction time, which were 100% HMF conversion rate and 85% DMF yield. Also, to compare the catalyst activity with those in the literature, recent reports on the use of copper-based catalysts for the hydrogenation of HMF to DMF are summarized in Table S3.[17,18,33,45−50] As shown in Table S3, the catalyst synthesized in this study achieved an excellent DMF yield after a short reaction time at a relatively low temperature. The Co_{20}-Cu@C catalyst prepared by pyrolysis of MOF has a highly porous structure, and the active components of the catalyst are highly dispersed. When materials are highly porous, the diffusion rates of the substrates and the products are likely to be faster than the catalytic rate.

Role of Cobalt in the Selective Hydrogenation of HMF. The process of HMF hydrogenation to DMF can be simplified in the following two steps: (1) the hydrogenation of aldehyde groups on HMF (C═O bond) and (2) the hydrogenation of hydroxymethyl groups on intermediate products such as DHMF (C−O bond of the hydroxyl

https://doi.org/10.1021/acsomega.1c00676
ACS Omega 2021, 6, 10910−10920

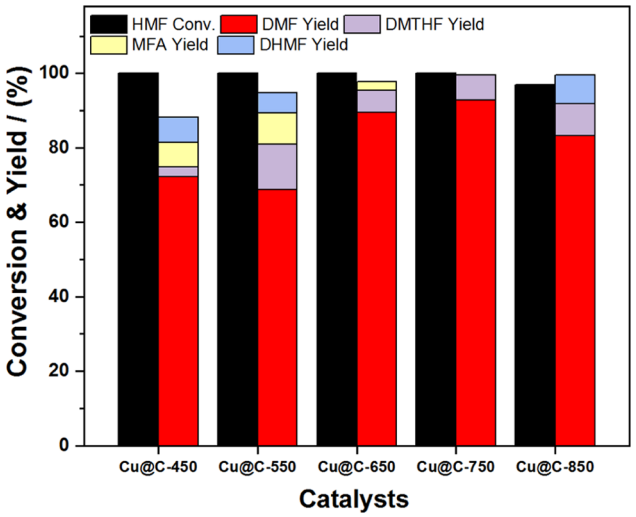

Figure 4. Effect of pyrolysis temperature on the 5-hydroxymethylfurfural (HMF) conversion and product yield. Reaction conditions: HMF loading, 0.5 g; catalyst loading, 0.1 g; IPA loading, 30 mL; hydrogen partial pressure, 3.0 MPa; *T*, 180 °C; time, 4 h; and agitation speed, 400 rpm.

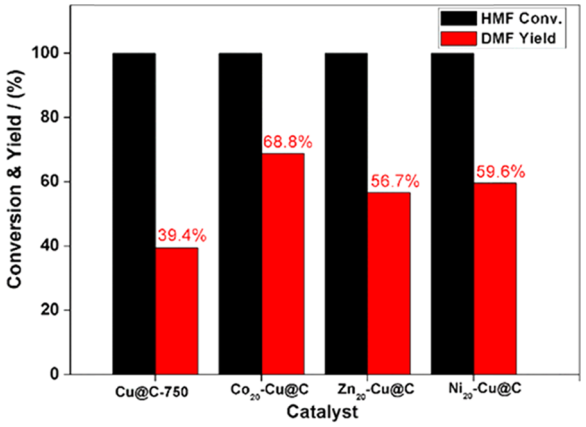

Figure 5. Effect of doping element on the HMF conversion and 2,5-dimethylfuran (DMF) yield. Reaction conditions: HMF loading, 0.5 g; catalyst loading, 0.1 g; IPA loading, 30 mL; hydrogen partial pressure, 2.5 MPa; *T*, 150 °C; time, 3 h; and agitation speed, 400 rpm.

group). In previous studies, the hydrogenation of the C−O bond (hydroxyl group) was found to be the rate-determining step for the hydrogenation of HMF to DMF.[19,51,52]

In the current study, the achieved catalytic performance was 100% HMF conversion for almost all catalysts, and the DMF yield was relatively large. The different DMF yields obtained by the catalyst were mainly for the different activities in catalyzing the hydrogenation of the C−O bond (hydroxyl group). Therefore, we assume that the cobalt doping may mainly increase the catalyst activity for the hydrogenation of the C−O bond (hydroxyl group), thereby increasing the DMF yield. To verify this assumption, an experiment was designed for research, as described below.

Furthermore, the catalysts before and after cobalt doping were used to evaluate the hydrogenation activities of 5-methylfurfural (MF) and 5-methylfurfuryl alcohol (MFA). The conversion rates of MF and MFA were determined by the hydrogenation activities of the catalyst for the C═O bond and the C−O bond (hydroxyl group), respectively. The catalytic

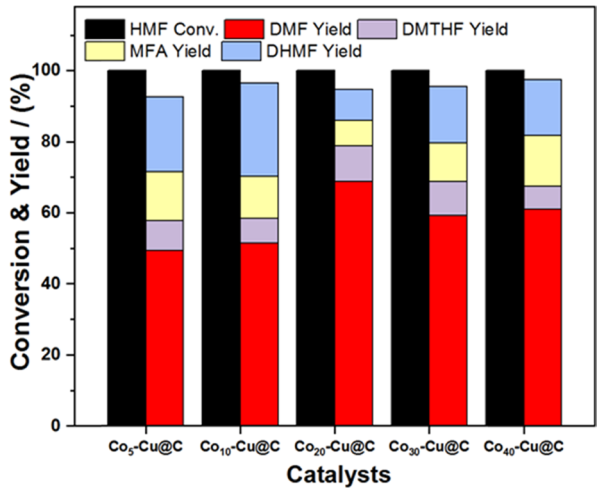

Figure 6. Effect of Co doping amount on the HMF conversion and DMF yield. Reaction conditions: HMF loading, 0.5 g; catalyst loading, 0.1 g; IPA loading, 30 mL; hydrogen partial pressure, 2.5 MPa; *T*, 150 °C; time, 3 h; and agitation speed, 400 rpm.

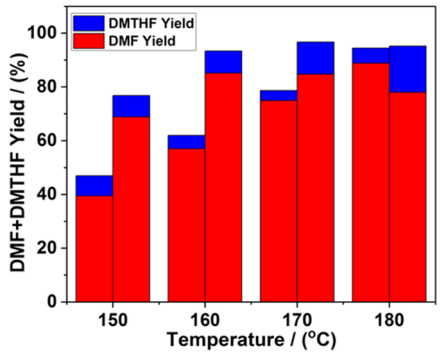

Figure 7. Effect of temperature on DMF and DMTHF yields over Cu@C-N750 (left column) and Co_{20}-Cu@C (right column) catalysts. Reaction conditions: HMF loading, 0.5 g; catalyst loading, 0.1 g; IPA loading, 30 mL; hydrogen partial pressure, 2.5 MPa; time, 3 h; and agitation speed, 400 rpm.

performance results are illustrated in Figure 8. In the MF hydrogenation activity test, the difference between the results of the two catalysts was small, while in the MFA hydrogenation activity test, the cobalt-doped catalyst showed a higher conversion rate. The experimental results confirm the above assumption that the difference in catalyst activity before and after cobalt doping is mainly reflected in the hydrogenation of the C−O bond (hydroxyl group), and the cobalt doping successfully modulates the hydrogenation activity of the catalyst for the C−O bond (hydroxyl group).

Based on the above structural characterization and catalytic test results, a possible reaction mechanism for the hydrogenolysis process of HMF to produce DMF is proposed (Scheme 2). For the dissociation of hydrogen, first, the hydrogen molecule may interact with the Cu^0 site on the catalyst, and then, the hydrogen molecule can be dissociated to form active hydrogen species. Subsequently, the carbonyl oxygen of HMF that has lone-pair electrons first adsorbs on the electrophilic Cu^0 site, which will promote the activation of the C═O bond. Then, the hydrogenation of the carbonyl group is induced by Cu particles in combination with the active hydrogen species, leading to the formation of DHMF. The electrophilic Cu^+ and CoO_x species, serving as Lewis acid sites,

https://doi.org/10.1021/acsomega.1c00676
ACS Omega 2021, 6, 10910−10920

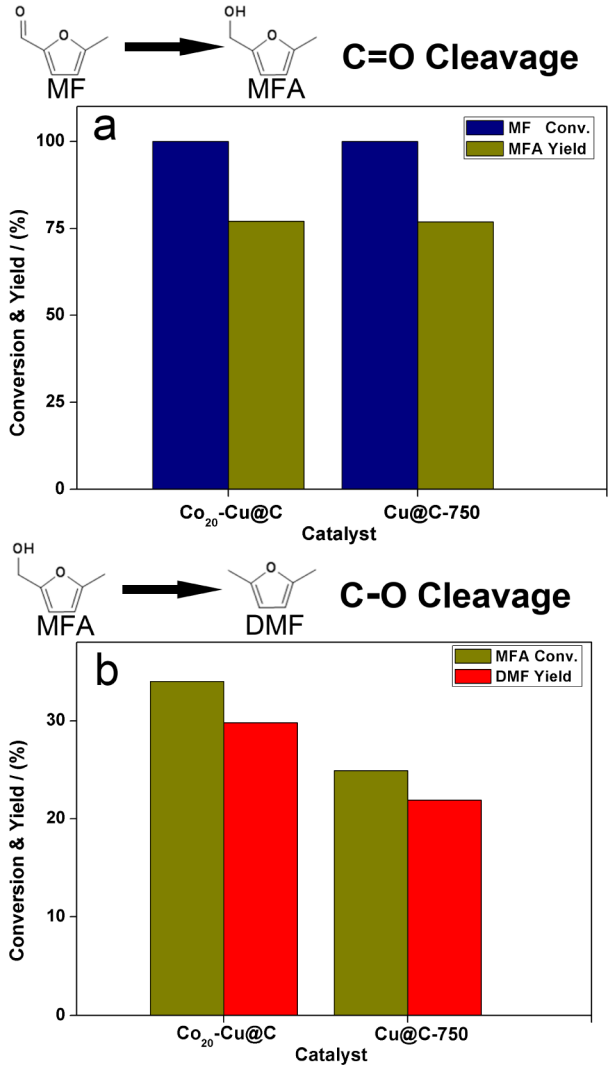

Figure 8. Reaction behaviors of (a) 5-methylfurfural (MF) and (b) 5-methylfurfuryl alcohol (MFA) over Co_{20}-Cu@C and Cu@C-750 catalysts. Reaction conditions: MF or MFA loading, 0.5 g; catalyst loading, 0.1 g; IPA loading, 30 mL; hydrogen partial pressure, 2.5 MPa; *T*, 140°C; time, 2 h; and agitation speed, 400 rpm.

can facilitate the polarization and activation of the C−O bond (hydroxyl group) in DHMF and MFA, leading to DMF production.[53,54] In the case of reaction route 1, Cu^+ species play a key role in the activation. However, according to our previous research,[29] Cu^+ is unstable during the reaction and is likely to be reduced. Therefore, the CoO_x species in reaction route 2 play an important role in maintaining a stable and high activity of the catalyst, especially in the C−O bond (hydroxyl group) hydrogenation.

Catalyst Recyclability. To study the reusability of the Co_{20}-Cu@C catalyst, the catalyst was subjected to multiple cycles. The cyclic performance results are shown in Figure 9a. The catalyst was subjected to five testing rounds, but the HMF conversion and DMF yield did not significantly reduce; this indicates that the catalyst has high stability and reusability. Interestingly, in the second round of reaction, the DMF yield increased slightly, which may be due to the weakening of the deep hydrogenation capacity of the recycled catalyst, preventing the deep hydrogenation of the target product DMF.

As shown in Figure 9b−d, the characterized results of the used catalyst had proven that the catalyst maintained a stable structure after the reaction. Compared with the characterized results of the fresh catalyst (Figures 1b, 2g,h, and 3c), the used one shows the same micromorphology and XRD results, indicating that the catalyst has high stability. In the high-resolution spectrum of Cu 2p, the peak weakening of Cu^{2+} might be on account of the reduction of Cu^{2+} during the reaction.

CONCLUSIONS

In this study, a copper−cobalt bimetallic catalyst derived from MOFs was synthesized and applied in the catalytic transfer hydrogenolysis of HMF to produce DMF. The catalyst showed excellent catalytic activity and selectivity under relatively mild reaction conditions without the participation of any precious metal. The cobalt doping did not significantly affect the chemical and physical environments of copper in the catalyst, suggesting that the cobalt was in situ loaded into the copper catalyst during the synthesis. The results of characterization tests indicated that the doped cobalt mainly existed as CoO_x. The results of the catalyst activity test showed that the CoO_x in the catalyst could effectively activate the C−O bond and

Scheme 2. Possible Mechanism of the Hydrogenolysis Process of HMF to Produce DMF through Two Reaction Routes

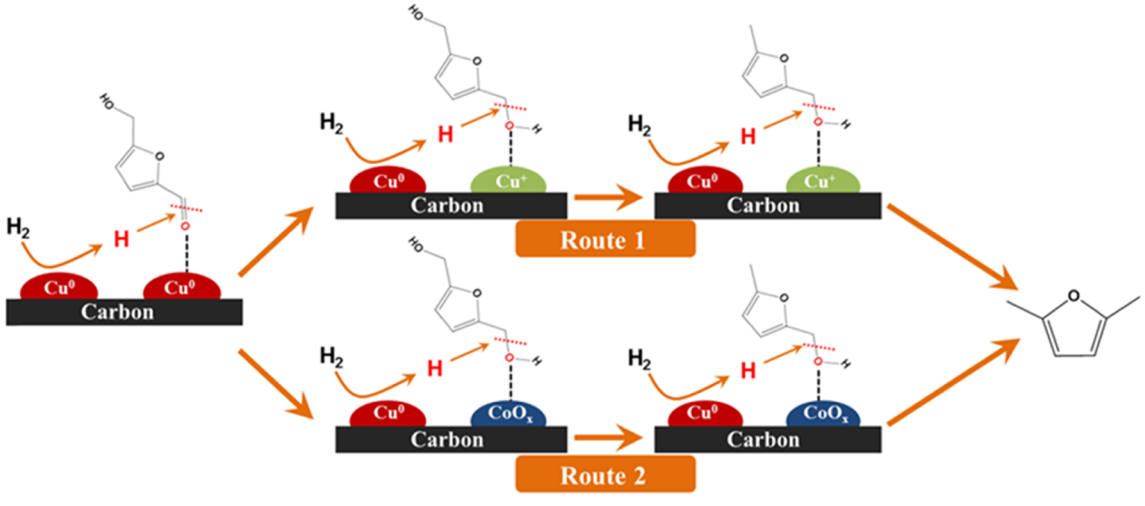

https://doi.org/10.1021/acsomega.1c00676
ACS Omega 2021, 6, 10910−10920

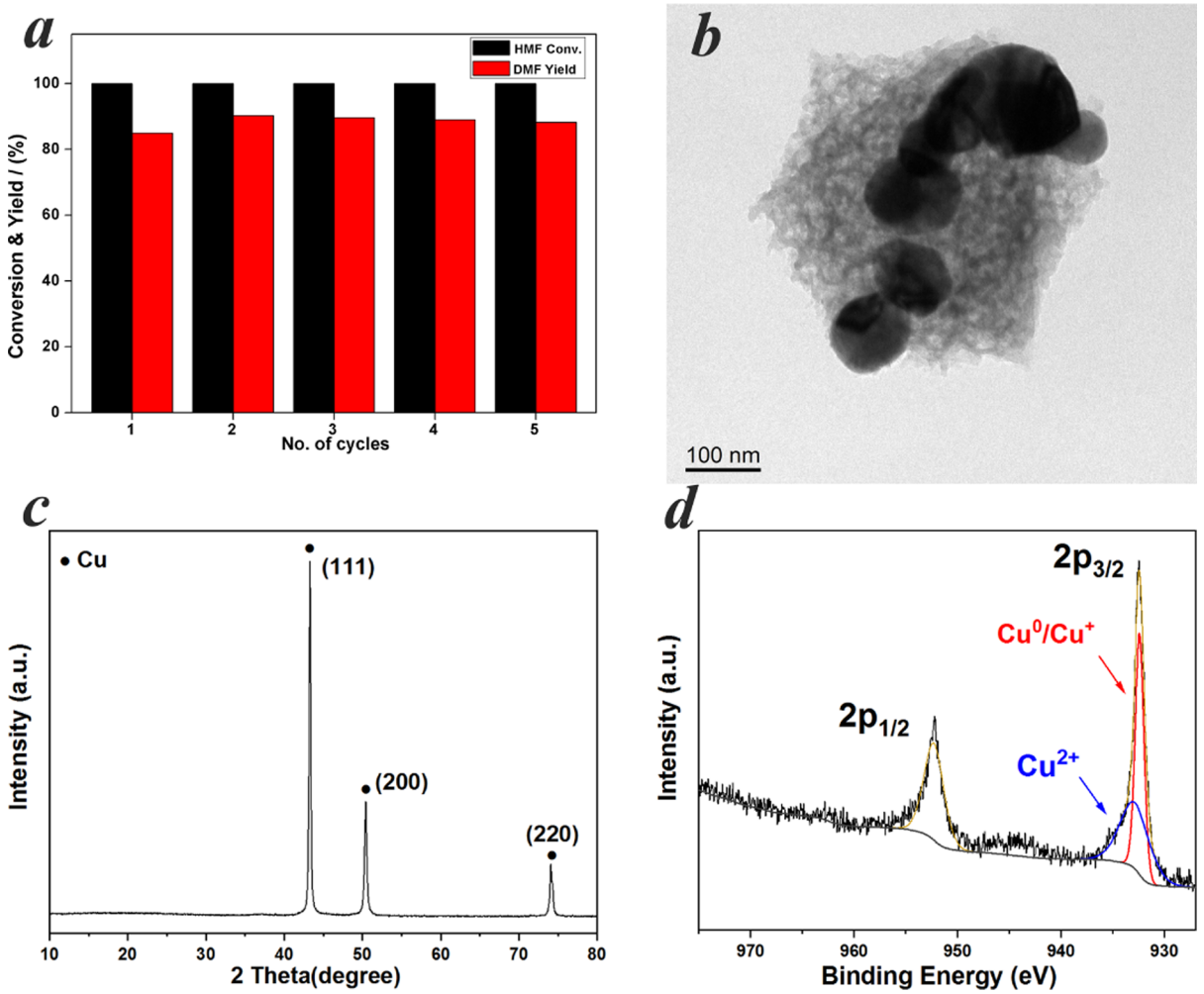

Figure 9. (a) Cyclic performance of the catalyst, (b) high-resolution transmission electron microscopy image, (c) X-ray diffraction patterns, and (d) high-resolution spectrum of Cu 2p of the used catalyst.

improve the hydrogenation activity of the catalyst. The remarkable catalytic activity of Co_{20}-Cu@C for the hydrogenation of HMF is attributed to the synergistic catalytic effect between Cu and CoO_x. Furthermore, the Co_{20}-Cu@C catalyst was used in the reaction under optimized reaction conditions, i.e., a reaction temperature of 160 °C, a hydrogen partial pressure of 2.5 MPa, and a reaction time of 3 h to obtain 100% HMF conversion and 85% DMF yield. More importantly, the catalyst activity did not decrease significantly after five rounds of testing, indicating that the catalyst has high stability. The presented copper−cobalt bimetallic catalyst provides a guiding principle and a reference value for the design of future non noble catalysts in the field of HMF conversion.

EXPERIMENTAL SECTION

Catalyst Synthesis Method. The Cu monometallic catalyst was synthesized by the static precipitation method. Typically, 10 mmol of BTC (1,3,5-benzenetricarboxylic acid) was dissolved in 100 mL of methanol, while 20 mmol of copper nitrate and 2 g of poly(vinyl pyrrolidone) (PVP) were dissolved in 100 mL of methanol. Then, BTC−methanol solution was slowly dropped into the metal nitrate solution with stirring. Subsequently, the blue mixed liquid was transferred to a round-bottom flask and kept at a constant temperature of 60 °C for 24 h in an oil bath. The blue precipitate was separated by filtration, washed with 100 mL of methanol three times, and dried in a vacuum oven to obtain the precursor powder. One gram of the precursor powder was measured and heated in a tube furnace under the protection of nitrogen, and the temperature was increased to the required temperature and kept constant for 4 h. Based on the pyrolysis temperature, the obtained catalyst is named Cu@C-X (X = 450, 550, 650, 750, and 850).

The method for synthesizing the precursor of the copper-based bimetallic catalyst is the same as above, except that the second metal nitrate (cobalt nitrate, zinc nitrate, or nickel nitrate) is additionally added, and all precursors of the bimetallic catalyst are pyrolyzed at 750 °C. The amount of second metal nitrate added is based on the molar ratio of copper nitrate. Based on the element and amount of doped metals, the catalyst is named M_x-Cu@C (M = doped metal element, x = second metal molar ratio).

Activity Test and Product Analysis. The catalytic performances in selective hydrogenation of the catalyst were carried out in a high-pressure autoclave. In a typical experiment, 0.5 g of the reaction substrates (HMF) and 0.1 g of the internal standard (toluene) were dissolved in 30 mL of isopropanol (IPA), the mixture was transferred to a stainless steel autoclave (100 mL) equipped with a mechanical agitator, and then 0.1 g of the catalyst was added. After sealing the

https://doi.org/10.1021/acsomega.1c00676
ACS Omega 2021, 6, 10910−10920

autoclave, H_2 was purged at least eight times to remove the air. Then, the autoclave was aerated with H_2 to the required pressure, and the temperature was increased according to the demand, while the mechanical agitation speed was modulated to 400 rpm. After a period of reaction, the autoclave was cooled to room temperature quickly. Finally, the solid catalyst and liquid product were separated using a centrifuge for the next experiment.

The qualitative and quantitative determination of liquid products is done by gas chromatography (Agilent 6820). The internal standard curve method was used for the quantification of the substrates and main products. In all cases, we have calculated that the respective carbon balances were above 90%.

To study the stability of the catalyst, the catalyst was subjected to multiple rounds of reaction. After the reaction, the catalyst was centrifuged, washed with ethanol three times, dried at 80 °C in vacuum for 2 h, and finally used for the next round of reaction without any additional treatment.

Catalyst Characterization. The inductively coupled plasma-optical emission spectroscopy (ICP-OES) was carried out on an Agilent 720ES. The Fourier transform infrared spectra of the samples were recorded on a PerkinElmer Spectrum 100 instrument (wave number 400−4000 cm^{-1}). X-ray diffraction (XRD) patterns of the prepared materials were recorded on a PANalytical PW3040/60 X-ray diffraction meter. The N_2 adsorption−desorption isotherms at 77 K were measured using a Micrometrics ASAP2460 instrument and calculated using the multipoint Brunauer−Emmett−Teller (BET) method. The field emission scanning electron microscopy (FESEM) image was taken on a JSM-7001F. The high-resolution transmission electron microscopy (HRTEM) image was obtained using an instrument JEOL JEM-2100F. X-ray photoelectron spectroscopy (XPS) spectra of the catalyst were recorded on a Thermo XPS ESCALAB 250Xi spectrometer equipped with a monochromatic Al Kα (1486.8 eV) X-ray source. Raman spectra were recorded on a LabRAM HR Evolution using an argon ion laser with an excitation wavelength of 532 nm.

■ ASSOCIATED CONTENT

Supporting Information

The Supporting Information is available free of charge at https://pubs.acs.org/doi/10.1021/acsomega.1c00676.

> X-ray diffraction patterns; infrared spectroscopy and electron microscopy characterizations of precursors; N_2 adsorption−desorption curve and textural parameters of catalysts; Raman spectra; effect of reaction time on the reaction; and comparison of the catalytic activity with other works (PDF)

■ AUTHOR INFORMATION

Corresponding Authors

Jianliang Zuo − *School of Chemistry & Chemical Engineering, Guangzhou University, Guangzhou 510006, Guangdong, China;* orcid.org/0000-0002-2000-3247; Email: jlzuo@hotmail.com

Zili Liu − *School of Chemistry & Chemical Engineering, Guangzhou University, Guangzhou 510006, Guangdong, China*; Email: gzdxlzl@163.com

Authors

Qingtu Zhang − *School of Chemistry & Chemical Engineering, Guangzhou University, Guangzhou 510006, Guangdong, China*

Lu Wang − *School of Chemistry & Chemical Engineering, Guangzhou University, Guangzhou 510006, Guangdong, China*

Feng Peng − *School of Chemistry & Chemical Engineering, Guangzhou University, Guangzhou 510006, Guangdong, China;* orcid.org/0000-0002-5154-6666

Shengzhou Chen − *School of Chemistry & Chemical Engineering, Guangzhou University, Guangzhou 510006, Guangdong, China;* orcid.org/0000-0001-7066-6412

Complete contact information is available at: https://pubs.acs.org/10.1021/acsomega.1c00676

Notes

The authors declare no competing financial interest.

■ ACKNOWLEDGMENTS

This work was supported by the National Natural Science Foundation of China [Grant numbers 22005070 and 21676060] and the Scientific Research Project of Guangzhou Municipal Colleges and Universities [Grant number 202032855].

■ REFERENCES

(1) Lelieveld, J.; Klingmueller, K.; Pozzer, A.; Burnett, R. T.; Haines, A.; Ramanathan, V. Effects of fossil fuel and total anthropogenic emission removal on public health and climate. *Proc. Natl. Acad. Sci., U.S.A.* **2019**, *116*, 7192−7197.

(2) Skovgaard, J.; van Asselt, H. The politics of fossil fuel subsidies and their reform: Implications for climate change mitigation. *Wires. Clim. Change.* **2019**, *10*, No. e581.

(3) Yang, X. J.; Hu, H.; Tan, T.; Li, J. China's renewable energy goals by 2050. *Environ. Dev.* **2016**, *20*, 83−90.

(4) Gautam, P.; Neha; Upadhyay, S. N.; Dubey, S. K. Bio-methanol as a renewable fuel from waste biomass: Current trends and future perspective. *Fuel* **2020**, *273*, No. 117783.

(5) Garedew, M.; Lin, F.; Song, B.; DeWinter, T. M.; Jackson, J. E.; Saffron, C. M.; Lam, C. H.; Anastas, P. T. Greener Routes to Biomass Waste Valorization: Lignin Transformation Through Electrocatalysis for Renewable Chemicals and Fuels Production. *ChemSusChem* **2020**, *13*, 4214−4237.

(6) Xu, C.; Paone, E.; Rodriguez-Padron, D.; Luque, R.; Mauriello, F. Recent catalytic routes for the preparation and the upgrading of biomass derived furfural and 5-hydroxymethylfurfural. *Chem. Soc. Rev.* **2020**, *49*, 4273−4306.

(7) Wang, H.; Zhu, C.; Li, D.; Liu, Q.; Tan, J.; Wang, C.; Cai, C.; Ma, L. Recent advances in catalytic conversion of biomass to 5-hydroxymethylfurfural and 2, 5-dimethylfuran. *Renewable Sustainable Energy Rev.* **2019**, *103*, 227−247.

(8) Fan, W.; Verrier, C.; Queneau, Y.; Popowycz, F. 5-Hydroxymethylfurfural (HMF) in Organic Synthesis: A Review of its Recent Applications Towards Fine Chemicals. *Curr. Org. Synth.* **2019**, *16*, 583−614.

(9) Menegazzo, F.; Ghedini, E.; Signoretto, M. 5-Hydroxymethylfurfural (HMF) Production from Real Biomasses. *Molecules* **2018**, *23*, No. 2201.

(10) Hu, L.; Lin, L.; Liu, S. Chemoselective Hydrogenation of Biomass-Derived 5-Hydroxymethylfurfural into the Liquid Biofuel 2,5-Dimethylfuran. *Ind. Eng. Chem. Res.* **2014**, *53*, 9969−9978.

(11) Qian, Y.; Zhu, L.; Wang, Y.; Lu, X. Recent progress in the development of biofuel 2,5-dimethylfuran. *Renewable Sustainable Energy Rev.* **2015**, *41*, 633−646.

(12) Saha, B.; Abu-Omar, M. M. Current Technologies, Economics, and Perspectives for 2,5-Dimethylfuran Production from Biomass-Derived Intermediates. *ChemSusChem* **2015**, *8*, 1133−1142.
(13) Kong, X.; Zhu, Y.; Fang, Z.; Kozinski, J. A.; Butler, I. S.; Xu, L.; Song, H.; Wei, X. Catalytic conversion of 5-hydroxymethylfurfural to some value-added derivatives. *Green Chem.* **2018**, *20*, 3657−3682.
(14) Nakagawa, Y.; Tamura, M.; Tomishige, K. Catalytic Reduction of Biomass-Derived Furanic Compounds with Hydrogen. *ACS Catal.* **2013**, *3*, 2655−2668.
(15) Sarkar, C.; Koley, P.; Shown, I.; Lee, J.; Liao, Y.-F.; An, K.; Tardio, J.; Nakka, L.; Chen, K.-H.; Mondal, J. Integration of Interfacial and Alloy Effects to Modulate Catalytic Performance of Metal-Organic-Framework-Derived Cu-Pd Nanocrystals toward Hydrogenolysis of 5-Hydroxymethylfurfural. *ACS Sustainable Chem. Eng.* **2019**, *7*, 10349−10362.
(16) Zu, Y.; Yang, P.; Wang, J.; Liu, X.; Ren, J.; Lu, G.; Wang, Y. Efficient production of the liquid fuel 2,5-dimethylfuran from 5-hydroxymethylfurfural over Ru/Co3O4 catalyst. *Appl. Catal., B* **2014**, *146*, 244−248.
(17) Brzezińska, M.; Keller, N.; Ruppert, A. M. Self-tuned properties of CuZnO catalysts for hydroxymethylfurfural hydrodeoxygenation towards dimethylfuran production. *Catal. Sci. Technol.* **2020**, *10*, 658−670.
(18) Esteves, L. M.; Brijaldo, M. H.; Oliveira, E. G.; Martinez, J. J.; Rojas, H.; Caytuero, A.; Passos, F. B. Effect of support on selective 5-hydroxymethylfurfural hydrogenation towards 2,5-dimethylfuran over copper catalysts. *Fuel* **2020**, *270*, No. 117524.
(19) Kumalaputri, A. J.; Bottari, G.; Erne, P. M.; Heeres, H. J.; Barta, K. Tunable and Selective Conversion of 5-HMF to 2,5-Furandimethanol and 2,5-Dimethylfuran over Copper-Doped Porous Metal Oxides. *ChemSusChem* **2014**, *7*, 2266−2275.
(20) Luo, J.; Monai, M.; Wang, C.; Lee, J. D.; Duchon, T.; Dvorak, F.; Matolin, V.; Murray, C. B.; Fornasiero, P.; Gorte, R. J. Unraveling the surface state and composition of highly selective nanocrystalline Ni-Cu alloy catalysts for hydrodeoxygenation of HMF. *Catal. Sci. Technol.* **2017**, *7*, 1735−1743.
(21) Gao, Z.; Li, C. Y.; Fan, G. L.; Yang, L.; Li, F. Nitrogen-doped carbon-decorated copper catalyst for highly efficient transfer hydrogenolysis of 5-hydroxymethylfurfural to convertibly produce 2,5-dimethylfuran or 2,5-dimethyltetrahydrofuran. *Appl. Catal., B* **2018**, *226*, 523−533.
(22) Zhao, H.; Jiang, Y.; Liu, H.; Long, Y.; Wang, Z.; Hou, Z. Direct synthesis of allyl alcohol from glycerol over CoFe alloy. *Appl. Catal., B* **2020**, *277*, No. 119187.
(23) Sun, Y.; Cai, Z.; Li, X.; Chen, P.; Hou, Z. Selective synthesis of 1,3-propanediol from glycidol over a carbon film encapsulated Co catalyst. *Catal. Sci. Technol.* **2019**, *9*, 5022−5030.
(24) Zhao, H.; Jiang, Y.; Chen, P.; Fu, J.; Lu, X.; Hou, Z. CoZn-ZIF-derived ZnCo2O4-framework for the synthesis of alcohols from glycerol. *Green Chem.* **2018**, *20*, 4299−4307.
(25) Sun, Y.; Li, X.; Cai, Z.; Bai, H.; Tang, G.; Hou, Z. Synthesis of 3D N-doped graphene/carbon nanotube hybrids with encapsulated Ni NPs and their catalytic application in the hydrogenation of nitroarenes. *Catal. Sci. Technol.* **2018**, *8*, 4858−4863.
(26) Venu, B.; Shirisha, V.; Vishali, B.; Naresh, G.; Kishore, R.; Sreedhar, I.; Venugopal, A. A Cu-BTC metal-organic framework (MOF) as an efficient heterogeneous catalyst for the aerobic oxidative synthesis of imines from primary amines under solvent free conditions. *New J. Chem.* **2020**, *44*, 5972−5979.
(27) Minh, T. T.; Phong, N. H.; Duc, H. V.; Khieu, D. Q. Microwave synthesis and voltammetric simultaneous determination of paracetamol and caffeine using an MOF-199-based electrode. *J. Mater. Sci.* **2018**, *53*, 2453−2471.
(28) Devarajan, N.; Karthik, M.; Suresh, P. Copper catalyzed oxidative homocoupling of terminal alkynes to 1,3-diynes: a Cu3(BTC)2 MOF as an efficient and ligand free catalyst for Glaser-Hay coupling. *Org. Biomol. Chem.* **2017**, *15*, 9191−9199.
(29) Zhang, Q. T.; Zuo, J. L.; Peng, F.; Chen, S. Z.; Wang, Q. Y.; Liu, Z. L. A Non-Noble Monometallic Catalyst Derived from Cu-MOFs for Highly Selective Hydrogenation of 5-Hydroxymethylfurfural to 2,5-Dimethylfuran. *Chemistryselect* **2019**, *4*, 13517−13524.
(30) Zhang, R.; Hu, L.; Bao, S.; Li, R.; Gao, L.; Li, R.; Chen, Q. Surface polarization enhancement: high catalytic performance of Cu/CuOx/C nanocomposites derived from Cu-BTC for CO oxidation. *J. Mater. Chem. A* **2016**, *4*, 8412−8420.
(31) Zuo, Z.-J.; Li, J.; Han, P.-D.; Huang, W. XPS and DFT Studies on the Autoxidation Process of Cu Sheet at Room Temperature. *J. Phys. Chem. C* **2014**, *118*, 20332−20345.
(32) Li, J.; Song, Z.; Hou, Y.; Li, Z.; Xu, C.; Liu, C.-L.; Dong, W.-S. Direct Production of 2,5-Dimethylfuran with High Yield from Fructose over a Carbon-Based Solid Acid-Coated CuCo Bimetallic Catalyst. *ACS Appl. Mater. Interfaces* **2019**, *11*, 12481−12491.
(33) Zhang, J.; Chen, J. Selective Transfer Hydrogenation of Biomass-Based Furfural and 5-Hydroxymethylfurfural over Hydrotalcite-Derived Copper Catalysts Using Methanol as a Hydrogen Donor. *ACS Sustainable Chem. Eng.* **2017**, *5*, 5982−5993.
(34) Kang, Y.; Park, J.; Kang, Y.-C. Surface characterization of CuSn thin films deposited by RF co-sputtering method. *Surf. Interface Anal.* **2016**, *48*, 963−968.
(35) Kwon, J.-D.; Kwon, S.-H.; Jung, T.-H.; Nam, K.-S.; Chung, K.-B.; Kim, D.-H.; Park, J.-S. Controlled growth and properties of p-type cuprous oxide films by plasma-enhanced atomic layer deposition at low temperature. *Appl. Surf. Sci.* **2013**, *285*, 373−379.
(36) Jian, J.; Kuang, D.; Wang, X.; Zhou, H.; Gao, H.; Sun, W.; Yuan, Z.; Zeng, J.; You, K.; Luo, H. a., Highly dispersed Co/SBA-15 mesoporous materials as efficient and stable catalyst for partial oxidation of cyclohexane with molecular oxygen. *Mater. Chem. Phys.* **2020**, *246*, No. 122814.
(37) Lima, T. M.; de Macedo, V.; Silva, D. S. A.; Castelblanco, W. N.; Pereira, C. A.; Roncolatto, R. E.; Gawande, M. B.; Zboril, R.; Varma, R. S.; Urquieta-Gonzalez, E. A. Molybdenum-promoted cobalt supported on SBA-15: Steam and sulfur dioxide stable catalyst for CO oxidation. *Appl. Catal., B* **2020**, *277*, No. 119248.
(38) Liu, N.; Tang, M. Q.; Jing, C. W.; Huang, W. Y.; Tao, P.; Zhang, X. D.; Lei, J. Q.; Tang, L. Synthesis of highly efficient Co3O4 catalysts by heat treatment ZIF-67 for CO oxidation. *J. Sol-Gel Sci. Technol.* **2018**, *88*, 163−171.
(39) Chen, K.; Bai, S. L.; Li, H. Y.; Xue, Y. J.; Zhang, X. Y.; Liu, M. C.; Jia, J. B. The Co3O4 catalyst derived from ZIF-67 and their catalytic performance of toluene. *Appl. Catal., A* **2020**, *599*, No. 117614.
(40) Zhu, K.; Zhang, M.; Feng, X.; Qin, L.; Kang, S.-Z.; Li, X. A novel copper-bridged graphitic carbon nitride/porphyrin nanocomposite with dramatically enhanced photocatalytic hydrogen generation. *Appl. Catal., B* **2020**, *268*, No. 118434.
(41) Liu, J.; Li, J.; He, S.; Sun, L.; Yuan, X.; Xia, D. Heterogeneous catalytic ozonation of oxalic acid with an effective catalyst based on copper oxide modified g-C3N4. *Sep. Purif. Technol.* **2020**, *234*, No. 116120.
(42) Lei, G.; Zhao, W.; Shen, L.; Liang, S.; Au, C.; Jiang, L. Isolated iron sites embedded in graphitic carbon nitride (g-C3N4) for efficient oxidative desulfurization. *Appl. Catal., B* **2020**, *267*, No. 118663.
(43) Wang, Y.; Shen, Y.; Zhao, Y.; Lv, J.; Wang, S.; Ma, X. Insight into the Balancing Effect of Active Cu Species for Hydrogenation of Carbon−Oxygen Bonds. *ACS Catalysis* **2015**, *5*, 6200−6208.
(44) Deutsch, K. L.; Shanks, B. H. Active species of copper chromite catalyst in C−O hydrogenolysis of 5-methylfurfuryl alcohol. *J. Catal.* **2012**, *285*, 235−241.
(45) Zhu, C.; Wang, H.; Li, H.; Cai, B.; Lv, W.; Cai, C.; Wang, C.; Yan, L.; Liu, Q.; Ma, L. Selective Hydrodeoxygenation of 5-Hydroxymethylfurfural to 2,5-Dimethylfuran over Alloyed Cu-Ni Encapsulated in Biochar Catalysts. *ACS Sustainable Chem. Eng.* **2019**, *7*, 19556−19569.
(46) Zhang, Z.; Yao, S.; Wang, C.; Liu, M.; Zhang, F.; Hu, X.; Chen, H.; Gou, X.; Chen, K.; Zhu, Y.; Lu, X.; Ouyang, P.; Fu, J. CuZnCoOx multifunctional catalyst for in situ hydrogenation of 5-hydroxymethylfurfural with ethanol as hydrogen carrier. *J. Catal.* **2019**, *373*, 314−321.

https://doi.org/10.1021/acsomega.1c00676
ACS Omega 2021, 6, 10910−10920

(47) Zhang, Z.; Wang, C.; Gou, X.; Chen, H.; Chen, K.; Lu, X.; Ouyang, P.; Fu, J. Catalytic in-situ hydrogenation of 5-hydroxymethylfurfural to 2,5-dimethylfuran over Cu-based catalysts with methanol as a hydrogen donor. *Appl. Catal., A* **2019**, *570*, 245−250.
(48) Sun, Y.; Xiong, C.; Liu, Q.; Zhang, J.; Tang, X.; Zeng, X.; Liu, S.; Lin, L. Catalytic Transfer Hydrogenolysis/Hydrogenation of Biomass-Derived 5-Formyloxymethylfurfural to 2, 5-Dimethylfuran Over Ni-Cu Bimetallic Catalyst with Formic Acid As a Hydrogen Donor. *Ind. Eng. Chem. Res.* **2019**, *58*, 5414−5422.
(49) Srivastava, S.; Jadeja, G. C.; Parikh, J. K. Optimization and Reaction Kinetics Studies on Copper-Cobalt Catalyzed Liquid Phase Hydrogenation of 5-Hydroxymethylfurfural to 2,5-Dimethylfuran. *Int. J. Chem. React. Eng.* **2018**, *16* (9), No. 20170197.
(50) Chen, B.; Li, F.; Huang, Z.; Yuan, G. Carbon-coated Cu-Co bimetallic nanoparticles as selective and recyclable catalysts for production of biofuel 2,5-dimethylfuran. *Appl. Catal., B* **2017**, *200*, 192−199.
(51) Zhang, Z.; Liu, C. W.; Liu, D.; Shang, Y. N.; Yin, X. Q.; Zhang, P.; Mamba, B. B.; Kuvarega, A. T.; Gui, J. Z. Hydrothermal carbon-supported Ni catalysts for selective hydrogenation of 5-hydroxymethylfurfural toward tunable products. *J. Mater. Sci.* **2020**, *55*, 14179−14196.
(52) Nakatsuka, K.; Yoshii, T.; Kuwahara, Y.; Mori, K.; Yamashita, H. Controlled Pyrolysis of Ni-MOF-74 as a Promising Precursor for the Creation of Highly Active Ni Nanocatalysts in Size-Selective Hydrogenation. *Chem. - Eur. J.* **2018**, *24*, 898−905.
(53) Li, D.; Liu, Q.; Zhu, C.; Wang, H.; Cui, C.; Wang, C.; Ma, L. Selective hydrogenolysis of 5-hydroxymethylfurfural to 2,5-dimethylfuran over Co3O4 catalyst by controlled reduction. *J. Energy Chem.* **2019**, *30*, 34−41.
(54) Yang, F.; Mao, J. B.; Li, S. M.; Yin, J. M.; Zhou, J. X.; Liu, W. Cobalt-graphene nanomaterial as an efficient catalyst for selective hydrogenation of 5-hydroxymethylfurfural into 2,5-dimethylfuran. *Catal. Sci. Technol.* **2019**, *9*, 1329−1333.

https://doi.org/10.1021/acsomega.1c00676
ACS Omega 2021, 6, 10910−10920